

Project Study: Tracking Drone Orientation with Multiple GPS Receivers

Zhan Zhang, *Student Member, IEEE*, and Danni Wu, *Student Member, IEEE*

I. INTRODUCTION

WITHOUT a good awareness of orientation and balance, a drone cannot effectively control its rotors to achieve desired flying status even hovering becomes impossible. A popular response is to install redundant inertial measurement units (IMU). IMU is an electronic device that measures and reports a body's specific force, angular rate, and the magnetic field surrounding the body, using a combination of accelerometers and gyroscopes, sometimes also magnetometers.

IMUs are typically used to maneuver aircraft, including unmanned aerial vehicles (UAVs), among many others, and spacecraft, including satellites and landers. Recent developments allow for the production of IMU-enabled GPS devices.[1]

An IMU allows a GPS receiver to work when GPS-signals are unavailable, such as in tunnels, inside buildings, or when electronic interference is present. Unfortunately, redundancy only addresses unreliable hardware. Various noise sources, including motor vibration, electromagnetic interference, and ambient ferromagnetic influences, create unreliability for the IMU. Worse even, the errors would accumulate through time and the IMUs are prone to various types of correlated failures.

This paper developed SafetyNet, which is a fail-safe mechanism for IMU failures. The basic idea is using multiple GPS to track 3D orientation of the UAV. The SafetyNet design includes 4 GPS receivers at four arms of the single drone upon IMU failure, this paper utilizes these GPS receivers to estimate the drone's 3D orientation.

As an alternative to the IMUs, SafetyNet uses GPS signals to estimate the real time orientation of the drone without any inertial or magnetometer assistance. Challenge comes that the traditional GPS system gets an error around 2-3 meters and the more advanced Differential GPS technology would still have a relative error in the scale of 10-20 centimeters (which equals to 20 degree in orientation). However, opportunities exist in relative GPS signal information and this paper utilizes the spatio-temporal information to achieve better accuracy.

The core additions of the SafetyNet, can be distilled as follows:

- Manipulating measurements across pairs of GPS receivers, satellites, and consecutive time points, capture 3D orientation from two different perspectives, which can institute transition model and measurement model of filters.
- GPS carrier-phase measurements can be used to achieve very precise positioning solutions. Carrier-phase measurements are much more precise than pseudorange measurements, but they are ambiguous by an integer number of cycles. The integer number of cycles is an unknown portion of GPS phase measurements, called integer ambiguity. In attempting to resolve this ambiguity, past work has adopted techniques akin to hard decoding, where the most likely state estimate is propagated across time. This paper designs the equivalent of soft decoding, whereby top-K possibilities of the ambiguity are propagated, each associated with an inferred probability. A particle filter is used to execute this idea the particle filter degenerating back into the Kalman Filter when the ambiguity is resolved confidently.
- This paper breaks away from the classical particle filter approach and adjusts the state of the particles based on available measurements. This speeds up convergence of the system, while requiring fewer particles (considerably reducing the computational complexity). As a result, the overall SafetyNet system lends itself to real time operation on today's drone hardware.[2]

II. PROBLEM FORMULATION

A. Drone Model

In this study, the drone is modeled with 4 GPS receivers installed on its 4 arms with a distance of 10 centimeters to the center. Therefore, a baseline matrix is generated as shown in figure 1 to model the ground truth relation between different receivers at different states.

The baseline matrix has the form:

$$B = \begin{bmatrix} \rho_{41} & \rho_{42} & \rho_{43} \end{bmatrix} \quad (1)$$

where ρ_{ij} is the vector between receiver i and j

$$\rho_{ij} = \rho_i - \rho_j \quad (2)$$

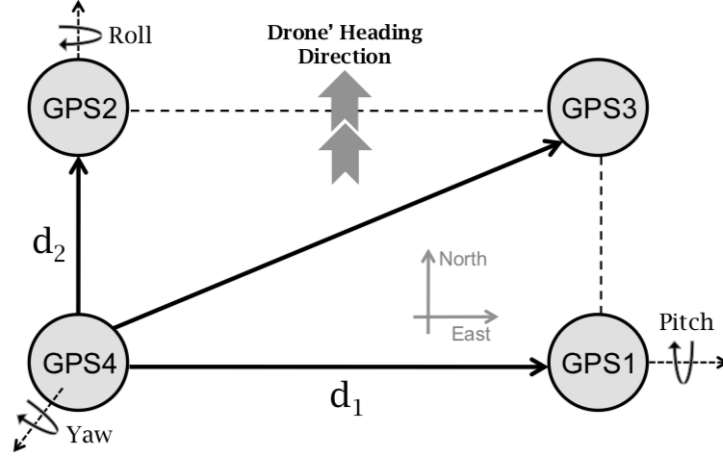


Fig. 1: Baseline Matrix

B. Pseudorange

Generally, the GPS operates in measuring the the time difference between transmitter and receive also the Pseudorange, which is the estimated distance between both ends is formed as in equation 3.

$$Pseudorange = ToF * c \quad (3)$$

where ToF is the time difference and c represents the speed of light.

However, when a satellite transmits a signal, it includes clock error as the starting time of transmission is obtained from its atomic clock. The reception time of the ground receiver is also recorded by less accurate local clock. Because the clock of a typical GPS receiver is not synchronized to the GPS satellites. The resulting error can be up to 300 km. GPS signal can get delayed when it enters the Earths atmosphere because of refractions in the Ionosphere and Troposphere. When signal passes through a multipath channel, more errors would be introduced. In this study, we model the error in pseudorange at receiver i from the satellite s as in equation 4.

$$Pseudorange_i^s = \rho_i^s + ct_i - ct^s + A^s + M_i + \epsilon_i^s \quad (4)$$

Here, ρ_i^s represents the real range, t_i and t^s stand for the clock error at the receiver and transmitter sides correspondingly. A models the interference by the atmosphere, M_i stands for the multipath interference and ϵ_i^s represents the hardware noise in measuring.

The operation error from the system would be as large as 1-4 meters which is far from satisfaction. Therefore, the Differential GPS technology is introduced leveraging the difference in signal phase and highly improves the system accuracy.

C. Differential GPS

The differential GPS technology leverages the phase of received GPS signals to improve the accuracy. One advantage of carrier phase is that its changes over time can be tracked reliably by utilizing the doppler shift in the signals.

The phase model is shown in equation 5 by ignoring the multipath and hardware noise error. Another advantage of carrier phase is that its changes over time can be tracked reliably by utilizing the doppler shift in the signal.

$$\lambda\phi_i^s = \rho_i^s + ct_i - ct^s + A^s - N_i^s \quad (5)$$

While N_i^s is Integer Ambiguity the number of whole cycles on the path from satellite to receiver.[3] The unknown property of N_i^s is called integer ambiguity solve from the phase measurement, and estimating the integer ambiguity is one of the major concern in the SafetyNet implementation. More discussion on integer ambiguity would come in later sections.

Environmental error sources in Equation 3 are correlated over short time periods and within small geographical areas (200 km). Thus, two GPS measurements across time can be subtracted (or differenced) to eliminate some of these factors. Similarly, simultaneous measurements from multiple GPS receivers can also be differenced. [4] This study propose 4 kind of differentials.

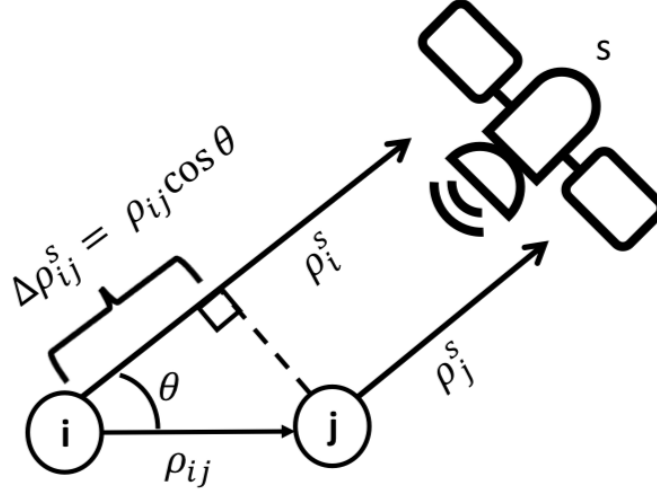


Fig. 2: $\lambda \Delta \phi_{ij}^s = \rho_{ij} \cdot \hat{l}_s + c \Delta t_{ij} - \lambda N_{ij}$

1) *Single Differential across Receivers ($SD_{ij}^s(t)$)*: Consider the carrier phase equations for two GPS receivers i and j from the same satellite s (let us ignore multipath and noise).

$$\begin{aligned} \lambda \Delta \phi_{ij}^s &= \phi_i^s - \phi_j^s \\ &= \Delta \rho_{ij}^s + c \Delta t_{ij} - \lambda N_{ij} \end{aligned} \quad (6)$$

By differencing the phases at different receivers, correlated error sources of atmospheric delays and satellite clock biases disappear.

For further simplification, $\Delta \rho_{ij}^s$ is replaced by $\rho_{ij} \cdot \hat{l}_s$, where ρ_{ij} is the vector between two receivers and \hat{l}_s is the line-of-sight unit vector from the receiver to the satellite. The transformation relationship is shown in figure 2.

The equation then become:

$$\lambda \Delta \phi_{ij}^s = \rho_{ij} \cdot \hat{l}_s + c \Delta t_{ij} - \lambda N_{ij} \quad (7)$$

While by single differential equation, some errors have disappeared, there still exists a function of the clock bias errors, $c \Delta t_{ij}$ still remains, this calls for the need for double differentials.

2) *Double Differential across Receivers and Satellites ($DD_{ij}^{sk}(t)$)*:

$$\begin{aligned} \lambda \nabla \Delta \phi_{ij}^{sk} &= \lambda \Delta \phi_{ij}^s - \lambda \Delta \phi_{ij}^k \\ &= \rho_{ij} \cdot (\hat{l}_s - \hat{l}_k) - \lambda \nabla \Delta N_{ij}^{sk} \end{aligned} \quad (8)$$

In this equation, i and j represent two different receivers, and k represents one satellite. Subtracting the single differential, we get double differential, the clock biases are removed and the absolute orientation is achieved, but the residue is polluted by integer ambiguity.

In this study, the spatio double differential forms our measurement model in the filtering process. This paper assumes the ambiguities are magically fixed, this provides us a reasonably precise estimate of relative positions between receiver pairs. The technology of Real Time Kinematics (RTK) technology can use the accurately known location of the reference receiver to calculate the location of the other.

3) *Single Differential across Time ($SD_i^s(t_{12})$)*: This paper also performs differentials across time for the same receiver. When there is no cycle slips, the equation can be listed as below,

$$\lambda \Delta \phi_i^s(t_{12}) = \rho_i(t_{12}) \cdot \hat{l}_s + c t_i(t_{12}) \quad (9)$$

Measurements across 4 satellites can help jointly estimate the relative displacement and clock bias. This estimated relative displacement is quite accurate since the integer ambiguity N_i^s does not included in it. This paper used a static receiver placed on the ground to verify the accuracy, and find that the estimation resulted in about 1cm/s of motion.

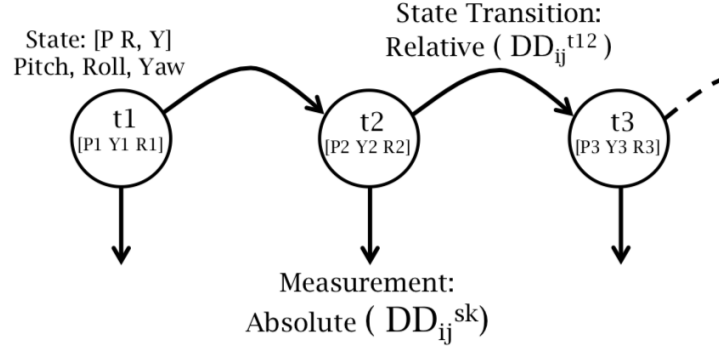


Fig. 3: System Model

4) *Double Differential across Receivers and Time* ($DD_{ij}^s(t_1 t_2)$): By taking the difference between the two single differentials across time, this paper achieved a measurement of the change in orientation, totally unpolluted by integer ambiguity. This measurement forms the system transition model in the filtering process. Under the no cycle slips assumption, the interger ambiguity can be eliminated by subtracting two equation of single differential across time.

$$\begin{aligned} \lambda \nabla \Delta \phi_{ij}^s(t_{12}) &= \lambda \Delta \phi_i^s(t_{12}) - \lambda \Delta \phi_j^s(t_{12}) \\ &= (\rho_{ij}(t_1) - \rho_{ij}(t_2)) \cdot \hat{l}_s + c \Delta t_{ij}(t_{12}) \end{aligned} \quad (10)$$

III. SYSTEM MODEL

SafetyNet treat model orientation tracking as a state estimation problem, where the state is defined as 3D orientation and represent by quaternion. With both the temporal and spatial differentials, we are able to model the orientation estimation problem by forming the transition state and absolute measurements. The system diagram is provided in figure 3.

1) *Transition State*: The temporal differential provides an accurate estimation upon the transition state as the integer ambiguity is cancelled. By minimizing the relative clock error, we can solve the equation to track the orientation change δq between states. Here we introduced the 3-dimensional vector representation of orientation $\delta \theta$ whose magnitude is the angle it rotates and direction is the axis it rotates around. By changing the representation metric, we are able to get rid of the constraint from quaternion and the estimation becomes a simple Least Square problem:

$$\lambda \nabla \Delta \phi_{ij}^s(t_{12}) = \rho_{ij}(q_0) [A(q_1) \hat{l}_s]_{\times} \delta \theta + c \Delta t_{ij}(t_{12}) \quad (11)$$

where $A(q)$ is the rotation matrix corresponding to the quaternion.

The solved $\delta \theta$ cannot be directly applied for transition state as the computation of rotation vector is not immuneable in large scale. We convert it back to quaternion form and the transition state becomes:

$$q_{k+1} = \delta q \otimes q_k \quad (12)$$

2) *Absolute State*: The spatial differential is transformed as our absolute measurement at each state.

$$\lambda \nabla \Delta \phi_{ij}^{sk} = \rho_{ij} \cdot (\hat{l}_s - \hat{l}_k) + \lambda \nabla \Delta N_{ij} \quad (13)$$

We can transform the measurement to a function of last state quaternion and a change in orientation in the vector form.

$$\lambda \nabla \Delta \phi_{ij}^{sk} - \rho_{ij}(q_0) A(q_n) \cdot (\hat{l}_s - \hat{l}_k) = \rho_{ij}(q_0) [A(q_n) \cdot (\hat{l}_s - \hat{l}_k)]_{\times} \delta \theta + \lambda \nabla \Delta N_{ij} \quad (14)$$

The measurement form would be further transformed in Extended Kalman Filter section for system linearization.

IV. ALGORITHMS

A. Extended Kalman Filter

Referring back to equation 12, the transition function is intrinsically a nonlinear operation (the quaternion multiplication), we make linearized approximations using Extended Kalman Filter (EKF). Now, linearizing transition model around the estimated rotation vector associated with quaternion q_k by applying Taylor Expansion, we have:

$$\delta \theta_{k+1} = F \delta \theta_k + \omega_k \quad (15)$$

where ω_k is the system noise.

With the linearization process, the absolute state is transformed from absolute rotation in form of quaternion to change in rotation vector ($\delta\theta$), as the rotation vector has the property of having muteable operation in small scales and removes the constraint in magnitude.

As with the transition function above, the measurement function can be written in the following form:

$$y_{k+1} - y_0 = H\delta\theta_{k+1} + v_{k+1} \quad (16)$$

where:

$$y = \lambda \nabla \Delta\phi_{ij}^{sk} - \lambda \nabla \Delta N_{ij} \quad (17)$$

$$y_0 = \rho_{ij}(q_0)A(q_n) \cdot (\hat{l}_s - \hat{l}_k) \quad (18)$$

$$H = \rho_{ij}(q_0)[A(q_n) \cdot (\hat{l}_s - \hat{l}_k)]_{\times} \quad (19)$$

and v_{k+1} is the measurement noise.

The above EKF has been designed under the convenient assumption that integer ambiguity and cycle slips have been resolved. However, this resolution is challenging, as evident from the numerous papers written on this topic.[5-7] The transition model and measurment model can now be combined using an Extended Kalman Filter for a refined estimate of θ^{k+1} .

In the measurement model, the integer ambiguity still exists. Here we make the assumption that the integer ambiguity is already solved such that we can ignore it for the filtering process and come back to it afterwards.

Once the drone is flying, additional multiples of wavelengths can also accumulate, called cycle slips. This paper first describe ways to mitigate the initial N and discuss cycle slips thereafter.

Therefore, this paper did not measure integer ambiguity directly, but make it as an index to identify the estimation they got is correct or not. Their core intuition is to compute a Cos function on the value of $2\pi N_{ij}^{sk}$, since N_{sk} should be an integer, $\text{Cos}(2\pi N_{sk}^{ij})$ should equal to 1.

The process of Kalman filtering is listed as below:

- Using transition model to get estimation of the next time point: $\delta\theta_{k+1}$.
- Using measurement model to get the estimation of integer ambiguity. In an ideal case, the correct q should make the corresponding values of N_{ij}^{sk} equal to 1.
- Identify the correctness of integer ambiguity using the summation of cosmetrics:

$$M(q) = \sum_{ij,sk} \cos(2\pi N_{sk}^{ij}) \quad (20)$$

and compare $M(q)$ to the number of possible combination pairs of receivers i, j and satellites s, k . If $M(q)$ approximates the number we consider it as correct and incorrect otherwise.

- If the integer ambiguity is correct, we can continue using kalman filter to estimate the state.
- If the integer ambiguity is not correct, the problem is transformed into a maximization problem. The cosmetic value would always be less than 1 if the estimated integer ambiguity is not an integer so our intention goes to find the best q to maximize $M(q)$, i.e.:

$$q_{coarse} = \underset{q}{\operatorname{argmax}} M(q) \quad (21)$$

- We simply perform a naive grid search in all 3 dimensions of ruler angle (yaw, pitch and roll) with a 5 degree step to find the optimized solution q_{coarse} to maximize the cosmetic value.
- After maximization, we update the previous q with q_{coarse} , and go back to step 2.

The system diagram is shown in figure 4.

B. Advanced Particle Filter

there exists one phenomenon called cycle slips, A cycle slips causes a jump in carrier-phase measurements when the receiver phase tracking loops experience a temporary loss of lock due to signal blockage or some other disturbing factor. It usually happens with highly aggressive flight drone. The process is listed as follows:

- Using kalman filtering, we can calculate the cosmetic of each q_i
- if the cosmetic is lower than one, which means the confidence is verified as low, we switch from kalman filter to particle filter to solve the integer ambiguity problem. We select K values of orientation q the values whose corresponding Cos metric ranks in the top-K. We initialize K particles(from grid search with the top k confidence in cosmetic form) at each of these orientation states and update them via the transition model and measurement model.
- All things goes well, however, there is one problem of the slow convergence of particle filter. To solve this, this paper developpe one advanced particle filter. In simple particle filter, we propagate to the next stage by transition model, and we

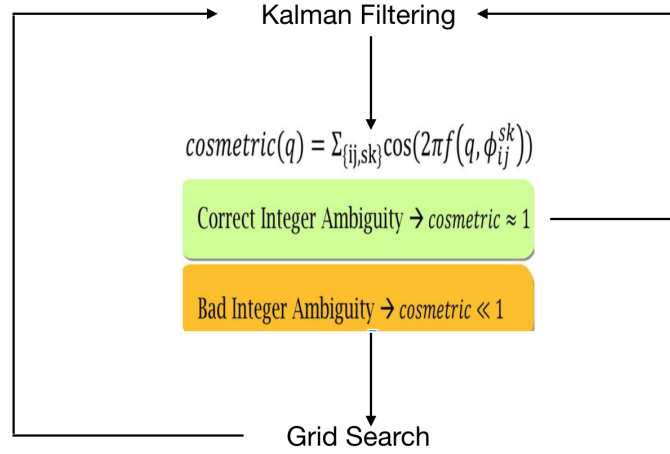


Fig. 4: Kalman Filter

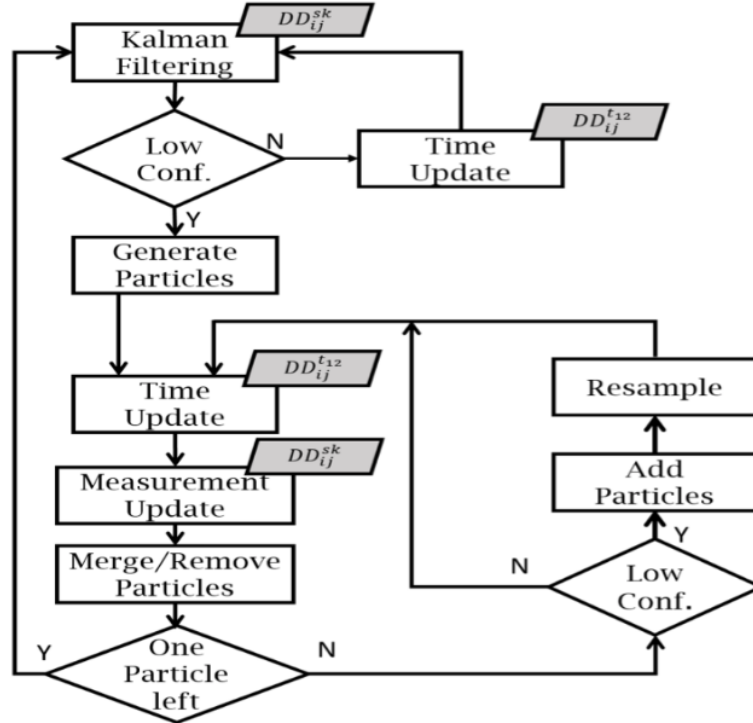


Fig. 5: Advanced Particle Filter

weight them by the measurement model, and assign probability for later use for filtering and so on. This paper make a simple modification, they move the particle to a state that maximizes the likelihood, and then perform the resampling step. Thus, the net outcome is faster convergence for the correct ambiguities, while disappearing particles for incorrect ambiguities.

- Upon its convergence, and if the cosmetric close to 1, we switch back to Kalman filter again. If the cosmetric is much lower than 1, more particles are added and resampled. Resampling is performed such that the resulting particles are an equal mix of the (highest weighted) current and new particles, and continuing the particle filtering process until the cosmetric close to one, and we go back to step one.

The system diagram is shown in figure 5.

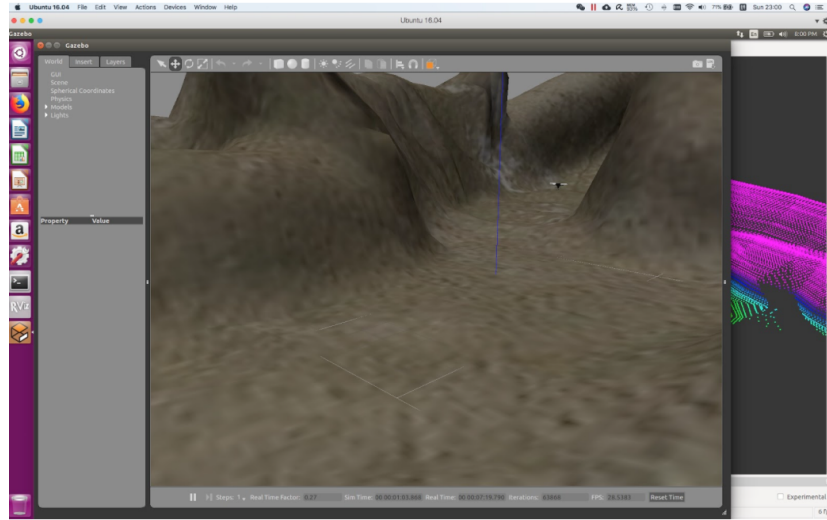


Fig. 6: Hector Quatercopter Simulation Platform

V. SIMULATION

A. Drone Simulation Platform

The simulation of the base drone is done based on Hector Quatercopter, an open-source implementation based on Robot Operation System (ROS) and Gazebo. The platform is shown in figure 6.

Ground truth data of the location and orientation data is collected to simulate the multiple GPS receivers attached to the drone. 4 GPS receivers are simulated on the 4 arms of the drone, rotated according to the ground truth orientation and shifted to the real location.

Two satellites are fixed on the Medium Earth Orbit and the phases are simulated from the corresponding distance between the satellite and the receiver.

As the drone's movement is relatively ignorable comparing to the distance to the satellites, the line-of-sight vector is considered as constant.

The Kalman and Advanced Particle filters are performed on the simulated data.

VI. REAL WORLD APPLICATIONS

With the booming applications with unmanned autonomos vechicle, reliable orientation estimation has been a nontrivial concern. SafetyNet proposes the novel algorithm to track the orientation with multiple GPS receivers to promise an error of 2 degrees in environment where magnetic interference and acceleration error accumulates.

The reliability and the accuracy of SafetyNet make it suitable in two major areas of applications.

a) Reliability: in the estimation makes it suitable for large quatercopters in aggressive flying status and in highly interfered magnetic field. Typical applications include flying in urban area (interference in magnetic field), obstacle avoidance in high speed flight (error in accelerometers), etc.

b) Accuracy: in orientation estimation powers up the accuracy in autonomos controll algorithms. For example, accurate tracking of the camera pose make it possible to achieve better vision-based antonomos flying. 3D reconstruction from the drone's lens is another application benefits from the accuracy.

VII. CONCLUSION

SafeNet use differential techniques, culminating in a novel particle filter framework running over multi-GNSS systems (GPS, GLONASS, and SBAS) to accurately computing the relative locations between each receiver pair, and translating these measurements into the drones 3D orientation. Results from 11 sessions of 5-7 minute flights report median orientation accuracies of 2 even under overcast weather conditions. The two filtering algorism used in the paper are Kalman filter and particle filter, we compared the performance of Kalman Filters and Advanced Particle Filter. The performance of Kalman Filters and Advanced Particle Filters is similar with less aggressive flight, when comes in to highly aggressive flight, Advanced Particle Filters can better track the drone than Kalman Filter. And after the highly aggressive flight, Kalman Fliter has large deviation, while Advanced Particle Filters still performs well. The reason can be listed as below:

- SafetyNet adopts a hybrid approach to satisfy the linearity and Gaussian assumptions required for Kalman Filter.

- Missing data in one or more of the receivers derails the state transition function.
- When the confidence is low, Kalman filter used "grid search" to find the best q_i , this method does not make use of the information from the previous time point and the following time point, and assume there is only one time point in the cycle slips period. In comparison, Advanced Particle Filters combines the information from the previous time point and the following time point, and do not forcefully assign there is only one time point in cycle slips period.

In conclusion, Advanced Particle Filters has better performance than Kalman Filters.